Analytical Classification of Dispersal Effects on Total Biomass in the Presence of a Weak Allee Effect

Bilel Elbetch

Analytical Classification of Dispersal Effects on Total Biomass in the Presence of a Weak Allee Effect

Bilel Elbetch
Faculty of Mathematics, University of Sciences and Technology Houari Boumediene, Algiers, Algeria.
E-mail address: elbetchbilal@gmail.com

October 2, 2025

Abstract

We investigate the impact of the weak Allee effect on the total biomass of a single species inhabiting a two-patch environment connected by asymmetric dispersal. In the proposed model, the first patch exhibits logistic growth, while the second patch follows a Nagumo-type growth law incorporating a weak Allee threshold. We establish the global existence, nonnegativity, and boundedness of solutions, and prove that the system admits a unique positive equilibrium that is globally asymptotically stable. Analytical results are derived for the asymptotic regime of high dispersal rates using singular perturbation theory, revealing an emergent weak Allee effect at the metapopulation scale. We conduct a complete classification of the parameter space to determine when dispersal increases, decreases, or has a unimodal effect on total equilibrium biomass, and provide geometric and monotonicity analyses of the equilibrium. Numerical simulations illustrate the theoretical trichotomy and highlight the ecological implications of dispersal management in fragmented landscapes. Our results generalize previous studies on logistic models to include the weak Allee effect, offering new insights into the interplay between dispersal intensity, asymmetry, and population persistence.

Mathematics Subject Classification: 37N25, 92D25, 34D23, 34D15.
Key words and phrases: Population dynamics, Weak Allee effect, Two-patch model, Asymmetric dispersal, Total biomass, Monotonicity analysis, Singular perturbation theory, Tikhonov's theorem.

Contents

1 Introduction

Population dynamics is a broad and active area of applied mathematics, addressing a variety of problems ranging from the persistence of species to the effects of environmental heterogeneity and migration. One classical question concerns the role of dispersal in shaping the long-term behaviour of populations in fragmented habitats. Comprehensive overviews of the mathematical and ecological aspects of such problems can be found in the works of Levin [22, 23] and Holt [20].

In many ecological situations, the spatial domain is best represented as a finite set of discrete habitat patches connected by migration pathways. Examples include archipelagos inhabited by bird populations and their predators, or networks of lakes connected by streams. Such discrete-space formulations fall within the framework of *insular biogeography*. From the mathematical side, the monograph of Levin, Powell, and Steele [24] provides a thorough account of patch-dynamics models, while Hanski and Gilpin [19] present a more ecological perspective. In this setting, the central mathematical question is to determine how dispersal influences global population abundance and persistence, and to understand the consequences of habitat fragmentation.

A seminal contribution in this direction is due to Freedman and Waltman [14], who in 1977 analysed the following two-patch logistic growth model with symmetric dispersal:

$$\begin{cases} \dfrac{dx_1}{dt} = r_1 x_1 \left(1 - \dfrac{x_1}{K_1}\right) + \varepsilon(x_2 - x_1), \\ \dfrac{dx_2}{dt} = r_2 x_2 \left(1 - \dfrac{x_2}{K_2}\right) + \varepsilon(x_1 - x_2), \end{cases} \tag{1.1}$$

where $x_i(t)$ denotes the population density in patch i, $r_i > 0$ is the intrinsic growth rate, $K_i > 0$ is the carrying capacity, and $\varepsilon \geq 0$ is the symmetric dispersal rate. They showed that, under certain conditions, the total equilibrium abundance may exceed the sum of the carrying capacities, $K_1 + K_2$. Holt [20] extended these ideas to source–sink systems. More recently, Arditi et al. [1] provided a complete mathematical analysis of (1.1) for symmetric dispersal.

In a subsequent work, Arditi et al. [2] generalised (1.1) to account for asymmetric dispersal

rates, leading to the model

$$\begin{cases} \dfrac{dx_1}{dt} = r_1 x_1 \left(1 - \dfrac{x_1}{K_1}\right) + \varepsilon(\gamma_{12} x_2 - \gamma_{21} x_1), \\ \dfrac{dx_2}{dt} = r_2 x_2 \left(1 - \dfrac{x_2}{K_2}\right) + \varepsilon(\gamma_{21} x_1 - \gamma_{12} x_2), \end{cases} \tag{1.2}$$

where $\gamma_{ij} > 0$ ($i \neq j$) are directional migration coefficients, and $\varepsilon\gamma_{12}$ (resp. $\varepsilon\gamma_{21}$) denotes the migration rate from patch 2 to patch 1 (resp. from patch 1 to patch 2). They observed that the positive equilibrium $(x_1^*(\varepsilon), x_2^*(\varepsilon))$ is the intersection of an ellipse and a parabola, and used a graphical method to characterise the regions of parameter space where dispersal is either beneficial or detrimental to total biomass.

Other variations of the two-patch logistic framework have been considered. Wu et al. [32] studied the asymmetric source–sink model

$$\begin{cases} \dfrac{dx_1}{dt} = r_1 x_1 \left(1 - \dfrac{x_1}{K_1}\right) + \varepsilon(x_2 - s x_1), \\ \dfrac{dx_2}{dt} = r_2 x_2 \left(-1 - \dfrac{x_2}{K_2}\right) + \varepsilon(s x_1 - x_2), \end{cases} \tag{1.3}$$

where $s > 0$ controls the dispersal asymmetry. They showed that depending on the magnitude of s, dispersal can increase, decrease, or even drive to extinction the total population, with clear thresholds separating these behaviours.

Dispersal effects have also been investigated in the presence of *Allee effects*, where the per-capita growth rate is reduced at low population densities. For example, Kang et al. [21] considered

$$\begin{cases} \dfrac{dx_1}{dt} = r_1 x_1 (x_1 - \theta)(1 - x_1) + \varepsilon(x_2 - x_1), \\ \dfrac{dx_2}{dt} = r_2 x_2 (x_2 - \theta)(1 - x_2) + \varepsilon(x_1 - x_2), \end{cases} \tag{1.4}$$

where θ is the Allee threshold. They showed that ε and θ strongly influence the global dynamics. Another model with an *additive* Allee effect was proposed by Chen et al. [3]:

$$\begin{cases} \dfrac{dx_1}{dt} = -x_1 + \varepsilon(\gamma_{12} x_2 - \gamma_{21} x_1), \\ \dfrac{dx_2}{dt} = x_2 \left(1 - x_2 - \dfrac{\sigma}{x_2 + a}\right) + \varepsilon(\gamma_{21} x_1 - \gamma_{12} x_2), \end{cases} \tag{1.5}$$

where $\sigma, a > 0$ are Allee-effect parameters. They distinguished between weak ($0 < \sigma < a$) and strong ($\sigma > a$) Allee effects, and demonstrated how changes in σ, a, and dispersal rates γ_{12}, γ_{21} can alter persistence and total biomass.

A substantial literature now exists on the interaction between dispersal and Allee effects in discrete-space models; see, for instance, [21, 25, 26, 27, 28, 30] for studies in discrete habitats, and [4, 5, 6, 7, 8, 9, 10, 11, 12, 13, 15, 18] for work on maximising total biomass in multi-patch environments. The present paper contributes to this line of research by incorporating a *weak* Allee effect in a two-patch logistic model with asymmetric dispersal, and by providing a complete analytical classification of how dispersal intensity influences total equilibrium biomass.

The paper is organized as follows. Section 1 introduces the ecological background and reviews related work. Section 2 presents the single-species dynamics with Allee effects. Section

3 formulates the two-patch model and establishes its basic properties, while Section 4 analyzes its equilibria and geometric structure. Section 5 studies the high-dispersal limit, and Section 6 classifies the effects of dispersal on total biomass. Section 7 provides a geometric interpretation, Section 8 illustrates the results with numerical simulations, and Section 9 concludes the paper.

2 Single-Species Dynamics with Allee Effects

We begin by considering a classical model that incorporates the Allee effect:

$$\frac{dx}{dt} = rx\left(1 - \frac{x}{K}\right)(x - M), \tag{2.1}$$

where $x(t)$ denotes the population density at time $t \geq 0$, and $r > 0$, $K > 0$, and $M \in \mathbb{R}$ are given parameters. The parameter r is the intrinsic growth rate, K is the environmental carrying capacity, and M represents the Allee threshold. We assume throughout that $M < K$.

The Allee effect describes a phenomenon where the per-capita growth rate is reduced at low population densities. Model (2.1) exhibits two qualitatively distinct types of Allee effects:

- A *weak Allee effect* occurs when $M \leq 0 < K$. In this case, the per-capita growth rate remains positive for all $x > 0$, and the population can grow from arbitrarily small densities.
- A *strong Allee effect* occurs when $0 < M < K$. In this setting, the population must exceed the critical threshold M to survive, otherwise it goes extinct.

These two cases are illustrated in Figure 1.

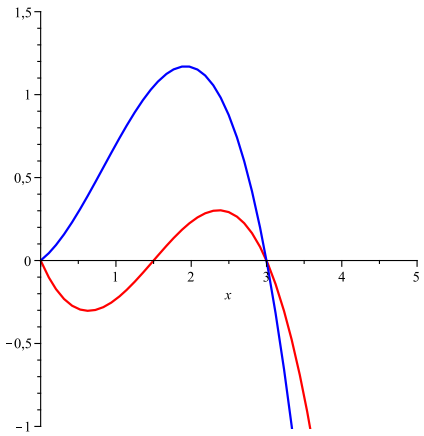

Figure 1: Population growth rate in model (2.1). The blue curve corresponds to a weak Allee effect with parameters $r = 0.7$, $K = 7$, and $M = -0.5$. The red curve corresponds to a strong Allee effect with $r = 0.7$, $K = 7$, and $M = 1.5$.

To understand the qualitative behavior of the system, we study the equilibria of (2.1). The right-hand side vanishes when $x = 0$, $x = M$, or $x = K$. Hence, the model admits:

- One or two positive equilibria depending on the value of M;
- Always the trivial equilibrium $x = 0$, representing extinction.

2.1 Case 1: Weak Allee Effect ($M \leq 0$)

In this case, all three equilibria $0 < M < K$ are ordered such that $x = 0$ is an equilibrium with *unstable* dynamics (since the growth rate is positive near the origin). The unique stable equilibrium on $\mathbb{R}_+$ is $x = K$, which is locally asymptotically stable (LAS). The population density always converges to K for any initial condition $x(0) > 0$, regardless of the magnitude of the Allee term.

2.2 Case 2: Strong Allee Effect ($0 < M < K$)

The dynamics are substantially different. In this case:

- $x = 0$ is a *locally stable* equilibrium (extinction state),
- $x = M$ is an *unstable* equilibrium (the Allee threshold),
- $x = K$ is a *locally asymptotically stable* equilibrium (saturation state).

The population converges to extinction if the initial population satisfies $x(0) < M$, and it converges to the carrying capacity K if $x(0) > M$. Therefore, the threshold M delineates the long-term survival of the species: it must be exceeded to escape extinction.

The qualitative behavior of system (2.1) can thus be summarized as follows:

- If $M < 0$, the Allee effect is weak, and every positive initial condition leads to persistence: $\lim_{t\to\infty} x(t) = K$.
- If $M > 0$, the Allee effect is strong, and extinction or survival depends on the initial condition:

$$\lim_{t\to\infty} x(t) = \begin{cases} 0, & \text{if } x(0) < M, \\ K, & \text{if } x(0) > M. \end{cases}$$

This threshold phenomenon under strong Allee effects has significant implications in conservation biology and population management, as small populations may face extinction purely due to insufficient initial density.

3 Mathematical Model and Preliminary Results

We consider a two-patch population model where the two patches are connected via asymmetric dispersal. The first patch exhibits logistic growth, while the second patch is subject to Allee effects as described in Equation (2.1). The resulting system of ordinary differential equations is given by:

$$\begin{cases} \dfrac{dx_1}{dt} = r_1 x_1 \left(1 - \dfrac{x_1}{K_1}\right) + \varepsilon\left(\gamma_{12} x_2 - \gamma_{21} x_1\right), \\ \dfrac{dx_2}{dt} = r_2 x_2 \left(1 - \dfrac{x_2}{K_2}\right)(x_2 - M) + \varepsilon\left(\gamma_{21} x_1 - \gamma_{12} x_2\right), \end{cases} \tag{3.1}$$

where $x_i(t)$ denotes the population density in patch $i \in \{1,2\}$ at time $t \geq 0$. The parameters $r_i > 0$ and $K_i > 0$ represent the intrinsic growth rate and the carrying capacity in patch i, respectively. The constant $M \in \mathbb{R}$ is the Allee threshold in patch 2, and we assume $M \leq 0 < K_2$, which corresponds to a weak Allee effect.

The parameter $\varepsilon > 0$ denotes the global dispersal rate, while the constants $\gamma_{12} > 0$ and $\gamma_{21} > 0$ quantify the directional migration rates from patch 2 to patch 1 and from patch 1 to patch 2, respectively. The migration is said to be symmetric when $\gamma_{12} = \gamma_{21}$.

We now address the basic properties of system (3.1), in particular the nonnegativity and boundedness of solutions. We show that the system is well-posed in the positive quadrant and that all trajectories remain uniformly bounded over time.

Proposition 3.1. *Let the initial condition $(x_1(0), x_2(0)) \in \mathbb{R}^2_+$. Then, the solution $(x_1(t), x_2(t))$ of system* (3.1) *remains nonnegative and uniformly bounded for all $t \geq 0$. Moreover, the set*

$$\Sigma = \left\{ (x_1, x_2) \in \mathbb{R}^2_+ \;\middle|\; x_1 + x_2 \leq \frac{\xi_2^*}{\xi_1^*} \right\},$$

where

$$\xi_1^* = \mu \min\{r_1, r_2(K_2 - M)\} \quad \text{and} \quad \xi_2^* = \mu \left(r_1 K_1 + r_2 K_2 (K_2 - M) \right),$$

is positively invariant and globally attracting.

Proof. Let us define the total population size $T(t) = x_1(t) + x_2(t)$. Summing the two equations in (3.1), the migration terms cancel, and we obtain:

$$\frac{dT}{dt}(t) = r_1 x_1(t) \left(1 - \frac{x_1(t)}{K_1}\right) + r_2 x_2(t) \left(1 - \frac{x_2(t)}{K_2}\right) (x_2(t) - M). \tag{3.2}$$

We now estimate the right-hand side from above. For any $x_1, x_2 \geq 0$, we have:

$$r_1 x_1 \left(1 - \frac{x_1}{K_1}\right) \leq r_1 (K_1 - x_1), \quad r_2 x_2 \left(1 - \frac{x_2}{K_2}\right) (x_2 - M) \leq r_2 (K_2 - M)(K_2 - x_2),$$

which yields:

$$\frac{dT}{dt}(t) \leq -\xi_1^* T(t) + \xi_2^*.$$

This differential inequality is linear and can be integrated explicitly to yield:

$$T(t) \leq \left(T(0) - \frac{\xi_2^*}{\xi_1^*} \right) e^{-\xi_1^* t} + \frac{\xi_2^*}{\xi_1^*}, \qquad \text{for all } t \geq 0. \tag{3.3}$$

In particular, this implies:

$$T(t) \leq \max\left\{ T(0), \frac{\xi_2^*}{\xi_1^*} \right\}, \qquad \forall t \geq 0,$$

which shows that both components $x_1(t)$, $x_2(t)$ remain bounded for all time.

Moreover, Equation (3.3) implies that the set $\Sigma \subset \mathbb{R}^2_+$ is positively invariant and attracts all trajectories, hence it is a global attractor for the dynamics of system (3.1). □

4 Equilibrium Analysis and Geometric Properties of the Two-Patch Model with Dispersal and Weak Allee Effect

In the absence of migration (i.e., when $\varepsilon = 0$), the system (3.1) admits (K_1, K_2) as a non-trivial equilibrium, which is locally asymptotically stable (LAS) in $\mathbb{R}^2_+$. The origin $(0,0)$ and the

boundary equilibria $(K_1,0)$ and $(0,K_2)$ are always unstable. For $\varepsilon > 0$, according to Theorem 6 in [11], the model (3.1) always has a unique positive equilibrium if $M \leq 0$, denoted by $E^*(\varepsilon) := (x_1^*(\varepsilon), x_2^*(\varepsilon))$, which is globally asymptotically stable in $\mathbb{R}^2_+ \setminus \{\mathbf{0}\}$.

Geometrically, the equilibrium of the system (3.1) corresponds to the solutions of the following algebraic system:

$$\begin{cases} 0 = r_1 x_1 \left(1 - \dfrac{x_1}{K_1}\right) + \varepsilon(\gamma_{12} x_2 - \gamma_{21} x_1), \\ 0 = r_2 x_2 \left(1 - \dfrac{x_2}{K_2}\right)(x_2 - M) + \varepsilon(\gamma_{21} x_1 - \gamma_{12} x_2). \end{cases} \tag{4.1}$$

The sum of the two equations in (4.1) reveals that the equilibrium points lie on a curve $\mathscr{C}$, whose equation is given by:

$$\mathscr{C}: \quad \Phi(x_1,x_2) := r_1 x_1 \left(1 - \frac{x_1}{K_1}\right) + r_2 x_2 \left(1 - \frac{x_2}{K_2}\right)(x_2 - M) = 0. \tag{4.2}$$

The curve $\mathscr{C}$, illustrated in red in Figure 3, passes through the points $(0,0)$, $(K_1,0)$, $(0,K_2)$, and $A := (K_1,K_2)$ when the Allee threshold parameter M is non-positive (see Figure 3). Notably, $\mathscr{C}$ is independent of the migration rate ε and the coefficients γ_{ij}.

If $M \leq 0$, the function $\Phi(x_1,x_2) = \Phi_1(x_1) + \Phi_2(x_2)$, where $\Phi_1(x_1) = r_1 x_1 \left(1 - \frac{x_1}{K_1}\right)$ and $\Phi_2(x_2) = r_2 x_2 \left(1 - \frac{x_2}{K_2}\right)(x_2 - M)$, is concave because both Φ_1 and Φ_2 are concave functions. Another key property of $\mathscr{C}$ is that if a point (x_1,x_2) lies on $\mathscr{C}$ with $x_1 < K_1$ (resp. $x_2 > K_2$), then $x_2 > K_2$ (resp. $x_1 < K_1$). In Figure 2, we plot $\mathscr{C}$ for various values of M.

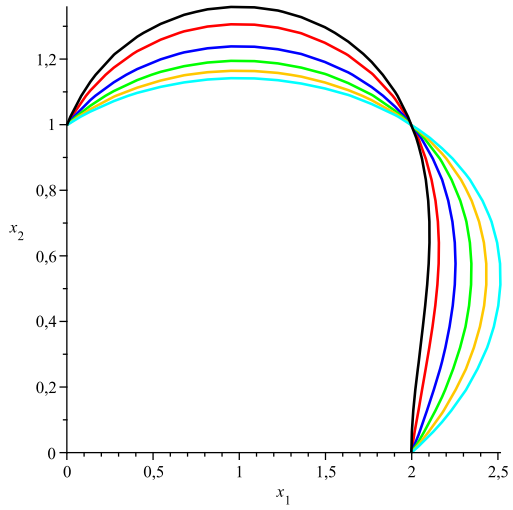

Figure 2: The curves $\mathscr{C}$ for $r_1 = 4$, $r_2 = 3$, $K_1 = 2$, $K_2 = 1$, and $M = 0$ (black curve), $M = -0.35$ (red curve), $M = -1$ (blue curve), $M = -1.65$ (green curve), $M = -2.3$ (orange curve), and $M = -2.95$ (cyan curve).

Solving the first equation of (4.1) for x_2 yields a parabola $\mathscr{P}_\varepsilon$, defined by the equation $x_2 = \varphi_\varepsilon(x_1)$, where φ_ε is given by:

$$\mathscr{P}_\varepsilon: \quad \varphi_\varepsilon(x_1) := \frac{1}{\gamma_{12}} \left(\gamma_{21} x_1 - \frac{r_1}{\varepsilon} x_1 \left(1 - \frac{x_1}{K_1}\right)\right). \tag{4.3}$$

The parabola $\mathscr{P}_\varepsilon$ (shown in blue in Figure 3 for various parameter values) depends on the migration rate ε. It always passes through the origin and the point $\mathscr{B} := \left(K_1, \frac{\gamma_{21}}{\gamma_{12}}K_2\right)$. Thus, the equilibrium points correspond to the non-negative intersections between $\mathscr{C}$ and $\mathscr{P}_\varepsilon$. Consequently, $E^*(\varepsilon)$ is determined by the intersection of $\mathscr{C}$ and $\mathscr{P}_\varepsilon$ (see Fig. 3) and satisfies:

$$\mathscr{C} \cap \mathscr{P}_\varepsilon : \quad \begin{cases} 0 = r_1 x_1^*(\varepsilon)\left(1 - \dfrac{x_1^*(\varepsilon)}{K_1}\right) + r_2 x_2^*(\varepsilon)\left(1 - \dfrac{x_2^*(\varepsilon)}{K_2}\right)(x_2^*(\varepsilon) - M), \\ x_2^*(\varepsilon) = \dfrac{1}{\gamma_{12}}\left(\gamma_{21}x_1^*(\varepsilon) - \dfrac{r_1}{\varepsilon}x_1^{*(\varepsilon)}\left(1 - \dfrac{x_1^*(\varepsilon)}{K_1}\right)\right). \end{cases}$$

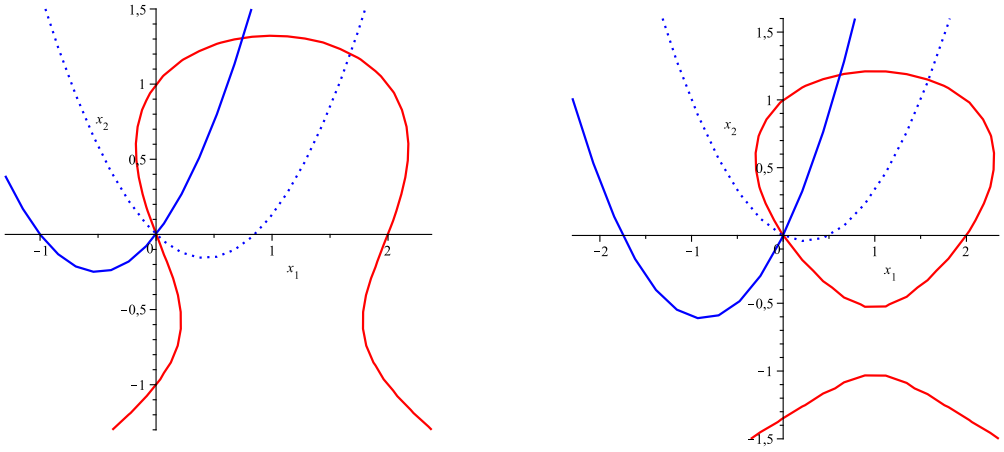

(Case a) (Case b)

Figure 3: Possible configurations of the curves $\mathscr{C}$ (red) and $\mathscr{P}_\varepsilon$ (blue, solid and dashed lines), where $r_1 = 5$, $r_2 = 3$, $K_1 = 2$, $K_2 = 1$, $\varepsilon = 1$, $\gamma_{12} = \gamma_{21} = 2$, and the Allee threshold parameter M is -1 for case (a) and -1.35 for case (b).

We define the **total equilibrium population** at the positive equilibrium under dispersal rate ε as:

$$T^*(\varepsilon) = x_1^*(\varepsilon) + x_2^*(\varepsilon), \tag{4.4}$$

representing the total asymptotic population abundance. For $\varepsilon = 0$, the total equilibrium population is:

$$T^*(0) = K_1 + K_2. \tag{4.5}$$

The primary objective of this paper is to investigate the influence of the weak Allee effect and dispersal on the total population size, and to conduct a comprehensive mathematical analysis of the two-patch model (3.1) across the full parameter space for $M \leq 0$.

5 Asymptotic Behavior of the Model under High Dispersal Rates

This section analyzes the asymptotic properties of System (3.1) as the migration rate becomes unbounded ($\varepsilon \to \infty$).

Theorem 5.1. *Let $E^*(\varepsilon)$ denote the positive equilibrium of System* (3.1)*. Then:*

$$\lim_{\varepsilon \to \infty} E^*(\varepsilon) = T^*(\infty)(u_1, u_2), \tag{5.1}$$

where $u_1 = \gamma_{12}/(\gamma_{12}+\gamma_{21})$, $u_2 = \gamma_{21}/(\gamma_{12}+\gamma_{21})$, *and* $T^*(\infty) = \lim_{\varepsilon\to\infty} T^*(\varepsilon)$ *with*

$$T^*(\infty) = K_1 + K_2 + \frac{-r_1u_1^2K_2 + r_2u_2^2K_1K_2 + r_2u_2^2K_1M - 2r_2u_2^3K_1(K_1+K_2) + \sqrt{\Delta}}{2r_2u_2^3K_1} \tag{5.2}$$

where $\Delta = \left(-\frac{r_1u_1^2}{K_1} + r_2u_2^2 + \frac{r_2u_2^2M}{K_2}\right)^2 + \frac{r_2u_2^3(r_1u_1 - r_2u_2M)}{K_2}$. *Moreover, under symmetric movement* ($\gamma_{12} = \gamma_{21}$)*:*

$$T^*(\infty) = K_1 + K_2 + \frac{-r_1K_2 + r_2K_1K_2 + r_2MK_1 - r_2K_1(K_1+K_2) + \sqrt{\Delta}}{r_2K_1}. \tag{5.3}$$

Proof. The equilibrium $E^*(\varepsilon)$ satisfies:

$$\begin{cases} r_1x_1^*(\varepsilon)\left(1 - \frac{x_1^*(\varepsilon)}{K_1}\right) + r_2x_2^*(\varepsilon)\left(1 - \frac{x_2^*(\varepsilon)}{K_2}\right)(x_2^*(\varepsilon) - M) = 0 \\ x_2^*(\varepsilon) = \frac{1}{\gamma_{12}}\left(\gamma_{21}x_1^*(\varepsilon) - \frac{r_1}{\varepsilon}x_1^*(\varepsilon)\left(1 - \frac{x_1^*(\varepsilon)}{K_1}\right)\right). \end{cases} \tag{5.4}$$

As $\varepsilon \to \infty$, System (5.4) reduces to:

$$\begin{cases} r_1x_1^*(\infty)\left(1 - \frac{x_1^*(\infty)}{K_1}\right) + r_2x_2^*(\infty)\left(1 - \frac{x_2^*(\infty)}{K_2}\right)(x_2^*(\infty) - M) = 0 \\ x_2^*(\infty) = \frac{\gamma_{21}}{\gamma_{12}}x_1^*(\infty). \end{cases} \tag{5.5}$$

Solutions to (5.5) include 0 and $E^*(\infty) = (x_1^*(\infty), x_2^*(\infty)) = T^*(\infty)(u_1,u_2)$. Convergence of $E^*(\varepsilon)$ to $E^*(\infty)$ follows by excluding the origin as a limit point. Specifically, for all $\varepsilon > 0$, there exists $i \in \{1,2\}$ such that $x_i^*(\varepsilon) > K_i$, ensuring $E^*(\varepsilon)$ is bounded away from 0. If $\gamma_{12}x_2^*(\varepsilon) < \gamma_{21}x_1^*(\varepsilon)$ for all $\varepsilon > 0$, then $r_2x_2^*(\varepsilon)(1 - x_2^*(\varepsilon)/K_2)(x_2^*(\varepsilon) - M) < 0$. Since $x_2^*(\varepsilon) > 0$ and $M \le 0$, we deduce $x_2^*(\varepsilon) > K_2$. Thus $E^*(\varepsilon) \to E^*(\infty)$ as $\varepsilon \to \infty$. The symmetric case (5.3) follows directly from (5.2) when $\gamma_{12} = \gamma_{21}$. □

Singular perturbation theory elucidates the system's behavior under perfect mixing ($\varepsilon \to \infty$):

Theorem 5.2. *Let* $(x_1(t,\varepsilon), x_2(t,\varepsilon))$ *solve System* (3.1) *with nonnegative initial conditions* (x_1^0, x_2^0). *As* $\varepsilon \to \infty$*:*

$$x_1(t,\varepsilon) + x_2(t,\varepsilon) = Z(t) + o_\varepsilon(1), \quad \textit{uniformly in } t \in [0,\infty) \tag{5.6}$$

and for any $t_0 > 0$*:*

$$\begin{cases} x_1(t,\varepsilon) = u_1Z(t) + o_\varepsilon(1) \\ x_2(t,\varepsilon) = u_2Z(t) + o_\varepsilon(1) \end{cases} \quad \textit{uniformly in } t \in [t_0,\infty), \tag{5.7}$$

where $Z(t)$ *satisfies:*

$$\begin{cases} \frac{dZ}{dt} = -\frac{r_2u_2^3}{K_2}Z^3 + \left(-\frac{r_1u_1^2}{K_1} + r_2u_2^2 + \frac{r_2u_2^2M}{K_2}\right)Z^2 + (r_1u_1 - r_2u_2M)Z \\ Z(0) = x_1^0 + x_2^0. \end{cases} \tag{5.8}$$

Proof. Define $X(t,\varepsilon) = x_1(t,\varepsilon) + x_2(t,\varepsilon)$. Rewriting (3.1) in (X, x_1)-coordinates yields:

$$\begin{cases} \dfrac{dX}{dt} = r_1 x_1 \left(1 - \dfrac{x_1}{K_1}\right) + r_2 (X - x_1)\left(1 - \dfrac{X - x_1}{K_2}\right)(X - x_1 - M) \\ \dfrac{dx_1}{dt} = r_1 x_1 \left(1 - \dfrac{x_1}{K_1}\right) + \varepsilon\left(\gamma_{12} X - (\gamma_{12} + \gamma_{21}) x_1\right). \end{cases} \tag{5.9}$$

As $\varepsilon \to \infty$, (5.9) becomes a slow-fast system with slow variable X and fast variable x_1. Rescaling time via $\tau = \varepsilon t$ gives the fast subsystem:

$$\frac{dx_1}{d\tau} = \frac{1}{\varepsilon} r_1 x_1 \left(1 - \frac{x_1}{K_1}\right) + \gamma_{12} X - (\gamma_{12} + \gamma_{21}) x_1.$$

Taking $\varepsilon \to \infty$ yields the fast dynamics:

$$\frac{dx_1}{d\tau} = \gamma_{12} X - (\gamma_{12} + \gamma_{21}) x_1. \tag{5.10}$$

The slow manifold is the set of equilibria of (5.10):

$$x_1^* = \frac{\gamma_{12}}{\gamma_{12} + \gamma_{21}} X = u_1 X. \tag{5.11}$$

As x_1^* is globally asymptotically stable (GAS) for (5.10), Tikhonov's theorem [29, 31] implies that after rapid attraction to the slow manifold, solutions of (5.9) are approximated by the reduced system obtained by substituting (5.11) into the X-dynamics:

$$\begin{aligned} \frac{dX}{dt} &= r_1 u_1 X \left(1 - \frac{u_1 X}{K_1}\right) + r_2 u_2 X \left(1 - \frac{u_2 X}{K_2}\right)(u_2 X - M) \\ &= -\frac{r_2 u_2^3}{K_2} X^3 + \left(-\frac{r_1 u_1^2}{K_1} + r_2 u_2^2 + \frac{r_2 u_2^2 M}{K_2}\right) X^2 + (r_1 u_1 - r_2 u_2 M) X. \end{aligned}$$

This recovers (5.8). Since (5.8) admits the GAS equilibrium $X^* = T^*(\infty)$ (given by (5.2)), Tikhonov's theorem guarantees approximations (5.6) and (5.7) hold uniformly for $t \in [0, \infty)$ and $t \in [t_0, \infty)$ ($t_0 > 0$), respectively. □

Under infinite dispersal, approximation (5.6) reveals that the total population follows a weak Allee effect (5.8). Consequently, as $t, \varepsilon \to \infty$, the total population $x_1(t,\varepsilon) + x_2(t,\varepsilon)$ converges to $T^*(\infty)$ (Theorems 5.1 and 5.2). Approximation (5.7) indicates that after a brief initial layer, population densities align with the proportions u_1 and u_2. Thus as $t, \varepsilon \to \infty$, $x_i(t,\varepsilon) \to u_i T^*(\infty)$ for $i = 1, 2$.

Under extreme dispersal rates ($\varepsilon \to \infty$), the system undergoes fundamental ecological reorganization. Rapid movement homogenizes the landscape, effectively merging distinct patches into a single well-mixed habitat where individuals lose spatial memory. Population densities stabilize at fixed proportions (u_1 and u_2) determined by the ratio of dispersal rates γ_{ij}, reflecting an equilibrium distribution across the landscape. Crucially, the total population exhibits a weak Allee effect (Eq. 5.8) - an emergent property arising from coupled local dynamics through dispersal that depresses per capita growth at intermediate densities. This transition occurs via a rapid redistribution phase where individuals reorganize according to dispersal ratios before settling into slow demographic trends. Ecologically, high connectivity eliminates patch-specific population identities, creates system-wide density dependence governed by parameter

averages, and enables rescue effects where productive patches sustain neighboring populations. Ultimately, intense dispersal transforms locally distinct populations into an integrated meta-population with collective dynamics governed by landscape-level processes rather than local conditions.

Let we consider the differential equation (5.8), We factorize the right-hand side as

$$\frac{dZ}{dt} = Z\Big(-AZ^2 + BZ + C\Big),$$

where

$$A = \frac{r_2 u_2^3}{K_2} > 0, \qquad B = -\frac{r_1 u_1^2}{K_1} + r_2 u_2^2 + \frac{r_2 u_2^2 M}{K_2}, \qquad C = r_1 u_1 - r_2 u_2 M.$$

Thus, $Z = 0$ is always an equilibrium. Nonzero equilibria satisfy

$$f(Z) := AZ^2 - BZ - C = 0,$$

with discriminant

$$\Delta = B^2 + 4AC.$$

If $\Delta \geq 0$, there are two real equilibria

$$Z_{\pm} = \frac{B \pm \sqrt{B^2 + 4AC}}{2A}.$$

The stability of $Z = 0$ is governed by

$$f'(0) = C = r_1 u_1 - r_2 u_2 M.$$

Hence

$$\begin{cases} Z = 0 \text{ is stable if } C < 0 \quad (\text{i.e. } r_1 u_1 < r_2 u_2 M), \\ Z = 0 \text{ is unstable if } C > 0. \end{cases}$$

For a nonzero equilibrium $Z^* > 0$, we compute

$$f'(Z^*) = Z^*(-2AZ^* + B).$$

Therefore, Z^* is stable if

$$Z^* > \frac{B}{2A}, \qquad \text{and unstable otherwise.}$$

- If $C > 0$, then $\Delta > B^2$ and there exists at least one positive root $Z_+ > 0$ which may be stable depending on the inequality $Z_+ > B/(2A)$.
- If $C < 0$, $Z = 0$ is stable and positive equilibria may or may not exist depending on Δ and the sign of $Z_{\pm}$, see figure 4.

6 Total equilibrium population

In this section, we analyze the effect of dispersal and weak Allee effect on the total equilibrium population for the system (3.1) and how the total biomass changes with dispersal rate. As in [15], for the two-patch logistic model (1.2), we present two complete classifications of the model parameter space, in each classification, we prove that exactly three cases can occur.

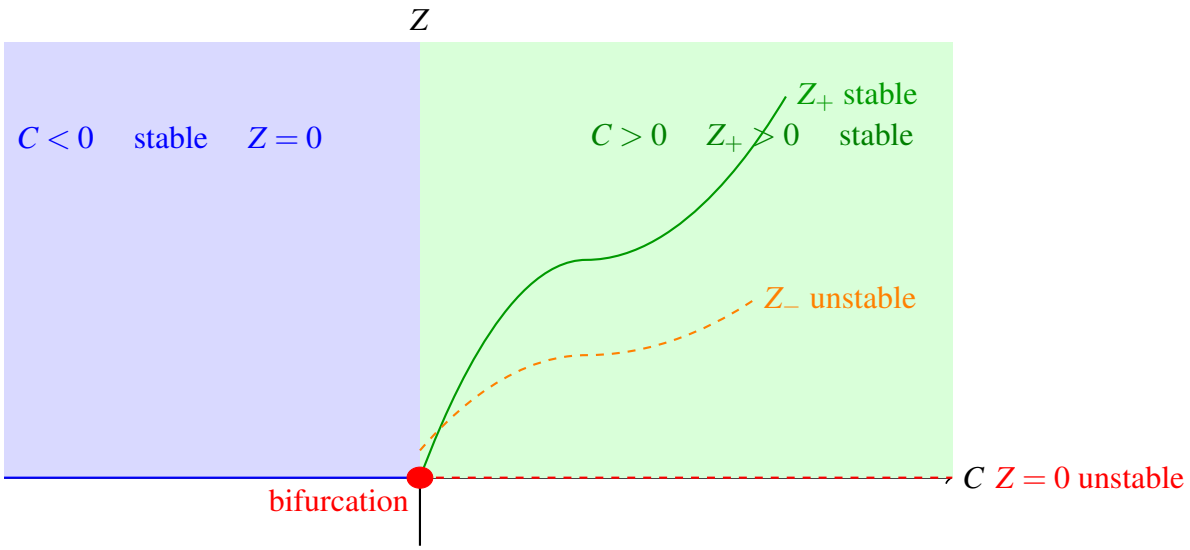

Figure 4: Enlarged bifurcation diagram with parameter C. For $C < 0$, only the trivial equilibrium $Z = 0$ exists and is stable (blue domain). At $C = 0$, a bifurcation occurs. For $C > 0$, the trivial state becomes unstable (red dashed line), and two positive equilibria appear: a stable branch Z_+ (green) and an unstable branch Z_- (orange).

6.1 Comparative Analysis of Equilibrium Populations at Varying Dispersal Rates

Arditi et al. [2] established a trichotomy for System (1.2) regarding the total equilibrium population $T^*(\varepsilon)$ relative to $K_1 + K_2$:

1. If $T^*(\infty) > K_1 + K_2$, then $T^*(\varepsilon) > K_1 + K_2$ for all $\varepsilon > 0$.
2. If $\frac{dT^*}{d\varepsilon}(0) > 0$ and $T^*(\infty) < K_1 + K_2$, there exists $\varepsilon_0 > 0$ such that:

$$\begin{aligned} T^*(\varepsilon) &> K_1 + K_2 \quad \text{for } 0 < \varepsilon < \varepsilon_0 \\ T^*(\varepsilon) &< K_1 + K_2 \quad \text{for } \varepsilon > \varepsilon_0 \\ T^*(\varepsilon_0) &= K_1 + K_2 \end{aligned}$$

3. If $\frac{dT^*}{d\varepsilon}(0) \leq 0$, then $T^*(\varepsilon) < K_1 + K_2$ for all $\varepsilon > 0$.

This implies $T^*(\varepsilon) = K_1 + K_2$ holds only at $\varepsilon = 0$ and at most one positive value ε_0, which exists iff $\frac{dT^*}{d\varepsilon}(0) > 0$ and $T^*(\infty) < K_1 + K_2$. Elbetch [6] generalized these results to the two-patch Richards model:

$$\begin{cases} \dfrac{dx_1}{dt} = r_1 x_1 \left[1 - \left(\dfrac{x_1}{K_1}\right)^{\mu}\right] + \varepsilon(\gamma_{12} x_2 - \gamma_{21} x_1) \\ \dfrac{dx_2}{dt} = r_2 x_2 \left[1 - \left(\dfrac{x_2}{K_2}\right)^{\mu}\right] + \varepsilon(\gamma_{21} x_1 - \gamma_{12} x_2) \end{cases} \tag{6.1}$$

for $\mu \neq 1$. We refer to [6] for detailed analysis of migration effects in Richards models.

Lemma 6.1. *The total equilibrium population satisfies:*

$$T^*(\varepsilon) = K_1 + K_2 + \varepsilon \left(\frac{K_1}{r_1 x_1^*(\varepsilon)} - \frac{K_2}{r_2 x_2^*(\varepsilon)(x_2^*(\varepsilon) - M)} \right) (\gamma_{12} x_2^*(\varepsilon) - \gamma_{21} x_1^*(\varepsilon)) \tag{6.2}$$

Proof. The equilibrium equations are:

$$\begin{cases} r_1 x_1^*(\varepsilon)\left(1-\dfrac{x_1^*(\varepsilon)}{K_1}\right) = -\varepsilon(\gamma_{12}x_2^*(\varepsilon)-\gamma_{21}x_1^*(\varepsilon)) \\ r_2 x_2^*(\varepsilon)\left(1-\dfrac{x_2^*(\varepsilon)}{K_2}\right)(x_2^*(\varepsilon)-M) = -\varepsilon(\gamma_{21}x_1^*(\varepsilon)-\gamma_{12}x_2^*(\varepsilon)) \end{cases} \tag{6.3}$$

Dividing the first equation by $\frac{r_1}{K_1}x_1^*(\varepsilon)$ and the second by $\frac{r_2}{K_2}x_2^*(\varepsilon)(x_2^*(\varepsilon)-M)$ yields:

$$\begin{cases} x_1^*(\varepsilon) = K_1 + \varepsilon\dfrac{\gamma_{12}x_2^*(\varepsilon)-\gamma_{21}x_1^*(\varepsilon)}{\frac{r_1}{K_1}x_1^*(\varepsilon)} \\ x_2^*(\varepsilon) = K_2 + \varepsilon\dfrac{\gamma_{21}x_1^*(\varepsilon)-\gamma_{12}x_2^*(\varepsilon)}{\frac{r_2}{K_2}x_2^*(\varepsilon)(x_2^*(\varepsilon)-M)} \end{cases}$$

Summing these equations gives (4.5). □

When $\gamma_{21}K_1 = \gamma_{12}K_2$, the ideal free distribution (IFD) holds: $(x_1^*(\varepsilon), x_2^*(\varepsilon)) \equiv (K_1, K_2)$ with $T^*(\varepsilon) = K_1 + K_2$ for all $\varepsilon \geq 0$. To exclude this trivial case, we assume throughout:

(H1) $\gamma_{21}K_1 > \gamma_{12}K_2$ $(K_1/u_1 > K_2/u_2)$

(H2) $\gamma_{21}K_1 < \gamma_{12}K_2$ $(K_1/u_1 < K_2/u_2)$

where $u_1 = \gamma_{12}/(\gamma_{12}+\gamma_{21})$, $u_2 = \gamma_{21}/(\gamma_{12}+\gamma_{21})$.

Proposition 6.2. *The equilibrium satisfies:*

- *Under (H1):* $\dfrac{K_1}{u_1} > \dfrac{x_1^*(\varepsilon)}{u_1} > \dfrac{x_2^*(\varepsilon)}{u_2} > \dfrac{K_2}{u_2}$ *and* $\gamma_{21}x_1^*(\varepsilon) > \gamma_{12}x_2^*(\varepsilon)$ *for all* $\varepsilon > 0$
- *Under (H2):* $\dfrac{K_1}{u_1} < \dfrac{x_1^*(\varepsilon)}{u_1} < \dfrac{x_2^*(\varepsilon)}{u_2} < \dfrac{K_2}{u_2}$ *and* $\gamma_{21}x_1^*(\varepsilon) < \gamma_{12}x_2^*(\varepsilon)$ *for all* $\varepsilon > 0$

Proof. Continuity and the equilibrium equations imply the sign consistency of $\gamma_{21}x_1^*(\varepsilon) - \gamma_{12}x_2^*(\varepsilon)$. Suppose equality holds at some $\tilde{\varepsilon} > 0$, then $(x_1^*(\tilde{\varepsilon}), x_2^*(\tilde{\varepsilon})) = (K_1, K_2)$, contradicting (H1) or (H2). From (6.3):

$$\begin{aligned} r_1 x_1^*(\varepsilon)\left(1-\frac{x_1^*(\varepsilon)}{K_1}\right) &= -r_2 x_2^*(\varepsilon)\left(1-\frac{x_2^*(\varepsilon)}{K_2}\right)(x_2^*(\varepsilon)-M) \\ &= \varepsilon(\gamma_{21}x_1^*(\varepsilon)-\gamma_{12}x_2^*(\varepsilon))\begin{cases} >0 & \text{under (H1)} \\ <0 & \text{under (H2)} \end{cases} \end{aligned}$$

Thus $x_1^*(\varepsilon) < K_1$ and $x_2^*(\varepsilon) > K_2$ under (H1), with reverse inequalities under (H2). □

Consequently, $\operatorname{sgn}(\gamma_{21}x_1^*(\varepsilon) - \gamma_{12}x_2^*(\varepsilon)) = \operatorname{sgn}(\gamma_{21}K_1 - \gamma_{12}K_2)$ for all $\varepsilon \geq 0$.

Proposition 6.3. *The derivative at* $\varepsilon = 0$ *is:*

$$\frac{dT^*}{d\varepsilon}(0) = (\gamma_{12}K_2 - \gamma_{21}K_1)\left(\frac{1}{r_1} - \frac{1}{r_2(K_2-M)}\right) \tag{6.4}$$

Thus $\frac{dT^*}{d\varepsilon}(0) = 0$ *iff* $r_1 = r_2(K_2-M)$ *or* $\gamma_{21}K_1 = \gamma_{12}K_2$.

Proof. Differentiating (6.3) yields:

$$\frac{d}{d\varepsilon}\begin{pmatrix}x_1^*\\ x_2^*\end{pmatrix} = \frac{\gamma_{21}x_1^* - \gamma_{12}x_2^*}{\nu(x_1^*,x_2^*)}\begin{pmatrix}\varepsilon\gamma_{21}\frac{x_1^*}{x_2^*} + \alpha_2 x_2^*(x_2^*-M) & \varepsilon\gamma_{12}\\ \varepsilon\gamma_{21} & \varepsilon\gamma_{12}\frac{x_2^*}{x_1^*} + \alpha_1 x_1^*\end{pmatrix}\begin{pmatrix}-1\\ 1\end{pmatrix} \tag{6.5}$$

where $\nu > 0$ and $\alpha_i = r_i/K_i$. Summing components gives:

$$\frac{dT^*}{d\varepsilon}(\varepsilon) = \frac{(\gamma_{21}x_1^* - \gamma_{12}x_2^*)}{\nu}\left(\alpha_1 x_1^* - \alpha_2 x_2^*(x_2^*-M) - \varepsilon\frac{x_1^*+x_2^*}{x_1^* x_2^*}(\gamma_{21}x_1^* - \gamma_{12}x_2^*)\right) \tag{6.6}$$

Evaluating at $\varepsilon = 0$ with $x_i^*(0) = K_i$ yields (6.4). □

Lemma 6.4. *If $T^*(\varepsilon_0) \le T^*(0)$ for some $\varepsilon_0 > 0$, then $\frac{dT^*}{d\varepsilon}(\varepsilon) < 0$ for all $\varepsilon \ge \varepsilon_0$. In particular, if $\frac{dT^*}{d\varepsilon}(0) < 0$, then $\frac{dT^*}{d\varepsilon}(\varepsilon) < 0$ for all $\varepsilon > 0$.*

Proof. From (4.5) and Proposition 6.2:

$$T^*(\varepsilon) - T^*(0) = \frac{\varepsilon}{\alpha_1\alpha_2 x_1^* x_2^*(x_2^*-M)}(\gamma_{21}x_1^* - \gamma_{12}x_2^*)\left(\alpha_1 x_1^* - \alpha_2 x_2^*(x_2^*-M)\right) \tag{6.7}$$

If $T^*(\varepsilon_0) \le T^*(0)$, (6.7) implies the product in (6.6) is negative. Since $\gamma_{21}x_1^* - \gamma_{12}x_2^* \neq 0$ by Proposition 6.2, we conclude $\frac{dT^*}{d\varepsilon}(\varepsilon_0) < 0$. □

Theorem 6.5. *For System* (3.1) *with $\gamma_{21}K_1 \neq \gamma_{12}K_2$:*

1. *If $\frac{dT^*}{d\varepsilon}(0) \le 0$, then $T^*(\varepsilon) \le T^*(0)$ for all $\varepsilon \ge 0$*
2. *If $\frac{dT^*}{d\varepsilon}(0) > 0$ and $T^*(\infty) \le T^*(0)$, there exists $\varepsilon_0 > 0$ such that:*

$$\begin{aligned} T^*(\varepsilon) &> K_1 + K_2 \quad \forall \varepsilon < \varepsilon_0\\ T^*(\varepsilon) &< K_1 + K_2 \quad \forall \varepsilon > \varepsilon_0\\ T^*(\varepsilon_0) &= K_1 + K_2 \end{aligned}$$

3. *If $T^*(\infty) \ge T^*(0)$, then $T^*(\varepsilon) \ge T^*(0)$ for all $\varepsilon > 0$*

Proof. Cases (1)-(3) follow from Lemma 6.4, continuity of T^*, and its differentiability near $\varepsilon = 0$. When $\frac{dT^*}{d\varepsilon}(0) = 0$ (i.e., $r_1 = r_2(K_2 - M)$ by Proposition 6.3):

- Under (H1): $\alpha_1 x_1^* - \alpha_2 x_2^*(x_2^*-M) < r_1 - r_2(K_2-M) = 0$
- Under (H2): $\alpha_1 x_1^* - \alpha_2 x_2^*(x_2^*-M) > r_1 - r_2(K_2-M) = 0$

Thus $T^*(\varepsilon) < T^*(0)$ for all $\varepsilon > 0$ in both cases, see figure 5. □

These results align with Theorem 4.2 in Gao [17], Theorem 4.5 in Gao and Lou [16], and Theorem 2.4 in Gao and Lou [15].

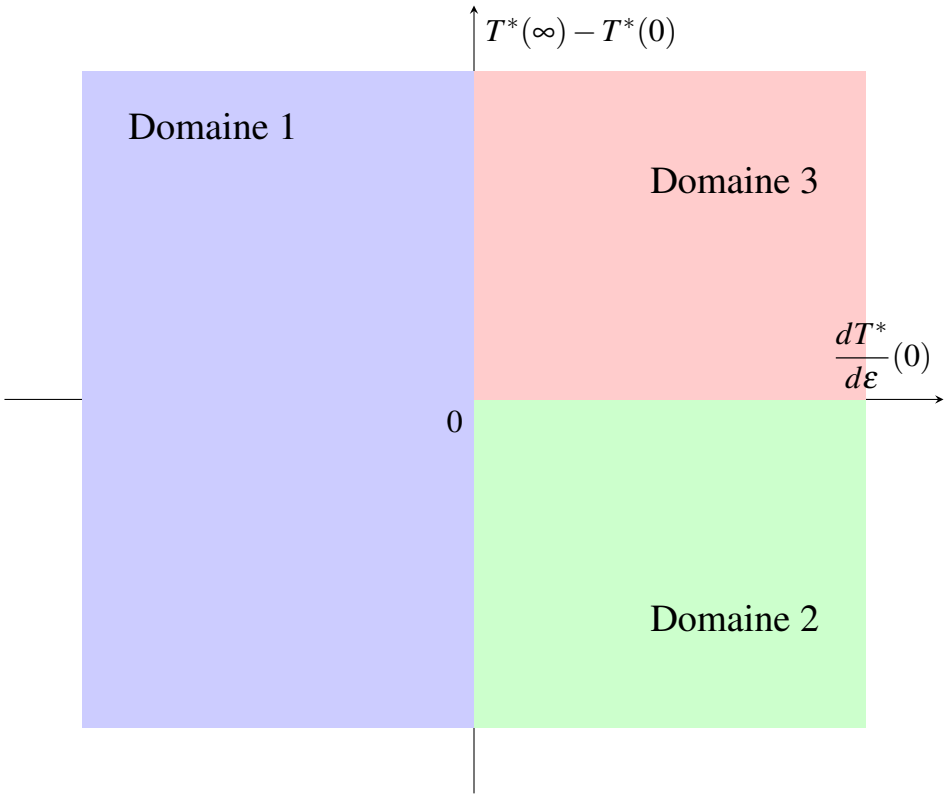

Figure 5: Illustration of the classification in Theorem 6.5. The plane is divided into colored domains according to the sign of the derivative $\frac{dT^*}{d\varepsilon}(0)$ (equation (6.4)) and the relative position of the asymptotic equilibrium $T^*(\infty)$ given by (5.2). Blue domain (Case 1): if $\frac{dT^*}{d\varepsilon}(0) \leq 0$, the total biomass satisfies $T^*(\varepsilon) \leq T^*(0)$ for all $\varepsilon \geq 0$. Green domain (Case 2): if $\frac{dT^*}{d\varepsilon}(0) > 0$ and $T^*(\infty) \leq T^*(0)$, there exists $\varepsilon_0 > 0$ such that $T^*(\varepsilon)$ is above the carrying capacity $K_1 + K_2$ for $\varepsilon < \varepsilon_0$, crosses it at $\varepsilon = \varepsilon_0$, and remains below it for $\varepsilon > \varepsilon_0$. Orange domain (Case 3): if $T^*(\infty) \geq T^*(0)$, then $T^*(\varepsilon) \geq T^*(0)$ for all $\varepsilon > 0$. The boundaries between domains are determined by the parameter combinations in $\gamma_{12}, \gamma_{21}, K_1, K_2, r_1, r_2, M$ entering $\frac{dT^*}{d\varepsilon}(0)$ and $T^*(\infty)$.

6.2 Monotonicity Analysis of the Total Equilibrium Population

Theorem 6.5 characterizes the position but not the monotonicity of $T^*(\varepsilon)$. To address this gap, we establish a complete classification analogous to Theorem 4.12 in Gao and Lou [16] and Theorem 2.5 in Gao and Lou [15]. The proof hinges on two key insights: 1. Critical points of $T^*(\varepsilon)$ on $[0,\infty)$ correspond to local maxima 2. For $\varepsilon \gg 1$, $\operatorname{sgn}\left(\frac{dT^*}{d\varepsilon}(\varepsilon)\right) = \operatorname{sgn}\left[(\gamma_{21}K_1 - \gamma_{12}K_2)\mathbb{T}'(\infty)\right]$ when $\mathbb{T}'(\infty) \neq 0$

Note that $\frac{dT^*}{d\varepsilon}(\infty) = \lim_{\varepsilon\to\infty}\frac{dT^*}{d\varepsilon}(\varepsilon) = 0$, but the asymptotic sign agrees with $\operatorname{sgn}\left(\frac{dT^*}{d\varepsilon}(\varepsilon)\right)$ for $\varepsilon \gg 1$. Here $\mathbb{T}'(\infty)$ is obtained by substituting equilibrium values $x_i^*(\infty)$ into:

$$\mathbb{T}'(\varepsilon) := \alpha_1 x_1^* - \alpha_2 x_2^*(x_2^* - M) - \varepsilon\frac{x_1^* + x_2^*}{x_1^* x_2^*}(\gamma_{21}x_1^* - \gamma_{12}x_2^*)$$

yielding:

$$\mathbb{T}'(\infty) = r_2(u_2T^*(\infty) - M) - r_1 + T^*(\infty)\left[2\alpha_1 u_1 - \alpha_2 u_2(1 + M + u_2T^*(\infty))\right] \tag{6.8}$$

where $T^*(\infty)$ is given in (4.4) and $\alpha_i = r_i/K_i$.

Lemma 6.6. *Under assumption (H1), if $\frac{dT^*}{d\varepsilon}(\tilde{\varepsilon}) = 0$ for some $\tilde{\varepsilon} > 0$, then $\frac{d^2T^*}{d\varepsilon^2}(\tilde{\varepsilon}) < 0$. Thus any critical point of $T^*(\varepsilon)$ on $\mathbb{R}_+$ is a local maximum.*

Proof. Differentiate the equilibrium sum equation:

$$r_1x_1^*\left(1 - \frac{x_1^*}{K_1}\right) + r_2x_2^*\left(1 - \frac{x_2^*}{K_2}\right)(x_2^* - M) = 0 \tag{6.9}$$

with respect to ε:

$$r_1\left(1 - \frac{2x_1^*}{K_1}\right)\frac{dx_1^*}{d\varepsilon} + r_2\left[\left(1 - \frac{x_2^*}{K_2}\right)(2x_2^* - M) - \frac{x_2^*}{K_2}(x_2^* - M)\right]\frac{dx_2^*}{d\varepsilon} = 0 \tag{6.10}$$

At a critical point $\tilde{\varepsilon}$, $\frac{dT^*}{d\varepsilon} = 0$ implies $\frac{dx_1^*}{d\varepsilon} = -\frac{dx_2^*}{d\varepsilon}$. Substituting into (6.10) gives either $\frac{dx_i^*}{d\varepsilon} = 0$ or:

$$\eta := r_1\left(1 - \frac{2x_1^*}{K_1}\right) = r_2\left[\left(1 - \frac{x_2^*}{K_2}\right)(2x_2^* - M) - \frac{x_2^*}{K_2}(x_2^* - M)\right] \tag{6.11}$$

Under (H1), $x_1^* < K_1$ implies $\eta < 0$. Differentiate (6.10) again:

$$\begin{aligned}
&r_1\left(1 - 2\frac{x_1^*(\varepsilon)}{K_1}\right)\frac{d^2x_1^*}{d\varepsilon^2}(\varepsilon) - 2\frac{r_1}{K_1}\left(\frac{dx_1^*}{d\varepsilon}(\varepsilon)\right)^2 + r_2\left(1 - \frac{x_2^*(\varepsilon)}{K_2}\right)(2x_2^*(\varepsilon) - M)\frac{d^2x_2^*}{d\varepsilon^2}(\varepsilon)\\
&+ (2r_2 + \frac{r_2}{K_2}M - 4\alpha_2x_2^*(\varepsilon))\left(\frac{dx_2^*}{d\varepsilon}(\varepsilon)\right)^2 - \frac{r_2}{K_2}x_2^*(\varepsilon)(x_2^*(\varepsilon) - M)\frac{d^2x_2^*}{d\varepsilon^2}(\varepsilon)\\
&- \frac{r_2}{K_2}(2x_2^*(\varepsilon) - M)\left(\frac{dx_2^*}{d\varepsilon}(\varepsilon)\right)^2 = 0,
\end{aligned}$$

At $\varepsilon = \tilde{\varepsilon}$ with $\frac{dx_i^*}{d\varepsilon} = 0$, this simplifies to:

$$\eta\frac{d^2T^*}{d\varepsilon^2} = \frac{2r_1}{K_1}\left(\frac{dx_1^*}{d\varepsilon}\right)^2 + \frac{2r_2}{K_2}(3x_2^* - M - K_2)\left(\frac{dx_2^*}{d\varepsilon}\right)^2$$

Since $M \leq 0$ and $x_2^* > K_2$ under (H1), the right-hand side is positive. With $\eta < 0$, we conclude $\frac{d^2T^*}{d\varepsilon^2} < 0$. □

Under (H1), Lemma 6.6 implies $T^*(\varepsilon)$ is either strictly decreasing, strictly increasing, or unimodal. The monotonicity type is determined by the signs of $\frac{dT^*}{d\varepsilon}(0)$ and $\mathbb{T}'(\infty)$:

Theorem 6.7. *Under assumption (H1):*

1. *If $\frac{dT^*}{d\varepsilon}(0) \leq 0$, then $T^*(\varepsilon)$ is strictly decreasing for all $\varepsilon > 0$*
2. *If $\frac{dT^*}{d\varepsilon}(0) > 0$ and $\mathbb{T}'(\infty) < 0$, there exists $\varepsilon_0 > 0$ such that:*

$$\frac{dT^*}{d\varepsilon}(\varepsilon) \begin{cases} > 0 & \varepsilon < \varepsilon_0 \\ = 0 & \varepsilon = \varepsilon_0 \\ < 0 & \varepsilon > \varepsilon_0 \end{cases}$$

3. *If $\mathbb{T}'(\infty) > 0$, then $T^*(\varepsilon)$ is strictly increasing for all $\varepsilon > 0$*

These mathematical classifications reveal how dispersal intensity mediates source-sink dynamics in metapopulations. When $\frac{dT^*}{d\varepsilon}(0) > 0$ (Case 2), moderate dispersal enhances total biomass by allowing surplus individuals from productive patches to colonize underutilized areas, creating a net rescue effect. Conversely, when $\frac{dT^*}{d\varepsilon}(0) \leq 0$ (Case 1), dispersal becomes detrimental as it draws individuals away from high-quality habitats faster than they can be replenished, effectively creating ecological traps. The critical threshold ε_0 represents the optimal dispersal rate that maximizes biomass before connectivity-induced homogenization reduces spatial complementarity. These patterns are particularly relevant in fragmented landscapes where dispersal management influences population persistence.

The monotonicity patterns characterize how connectivity regulates ecosystem productivity. Strictly increasing $T^*(\varepsilon)$ (Case 3) occurs when dispersal consistently improves resource exploitation across patches, typical of systems with strong source-sink asymmetry. The unimodal pattern (Case 2) reflects the connectivity paradox: initial dispersal benefits populations by enabling recolonization, but excessive movement suppresses local adaptation and creates synchrony that amplifies extinction risk. The critical threshold ε_0 marks the tipping point where dispersal shifts from beneficial to harmful. Strictly decreasing $T^*(\varepsilon)$ (Case 1) indicates fragile systems where any dispersal reduces biomass, characteristic of populations near extinction thresholds where emigration exacerbates decline. These dynamics underscore that conservation strategies must balance connectivity to maintain optimal dispersal regimes rather than maximize movement, see figure 6.

6.3 Linking the initial derivative to the infinite-diffusion regime

We now investigate the relation between the derivative of the total equilibrium biomass at $\varepsilon = 0$ and its limiting value $T^*(\infty)$ as $\varepsilon \to \infty$.

Recall from (6.4) that

$$\frac{dT^*}{d\varepsilon}(0) = (\gamma_{12}K_2 - \gamma_{21}K_1)\left(\frac{1}{r_1} - \frac{1}{r_2(K_2 - M)}\right). \tag{6.12}$$

Since $r_1 > 0$, $r_2 > 0$ and $K_2 - M > 0$, the sign of this derivative is determined by

$$\operatorname{sgn}\left(\frac{dT^*}{d\varepsilon}(0)\right) = \operatorname{sgn}\left(\gamma_{12}K_2 - \gamma_{21}K_1\right) \cdot \operatorname{sgn}\left(r_2(K_2 - M) - r_1\right).$$

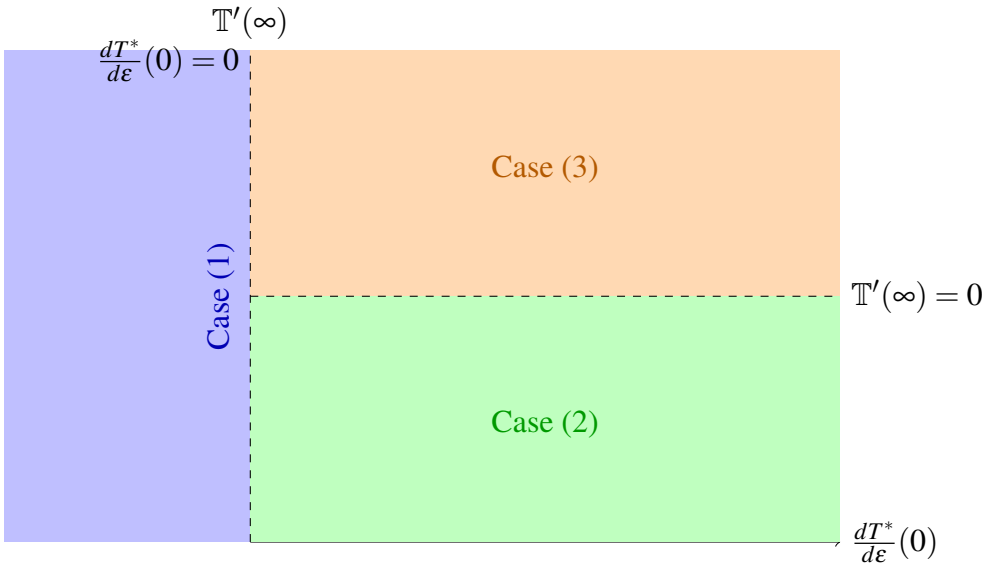

Figure 6: Classification of the monotonicity result in Theorem 6.7. Blue domain (Case 1): when $\frac{dT^*}{d\varepsilon}(0) \leq 0$, the total biomass $T^*(\varepsilon)$ is strictly decreasing for all $\varepsilon > 0$. Green domain (Case 2): if $\frac{dT^*}{d\varepsilon}(0) > 0$ and $\mathbb{T}'(\infty) < 0$, the function $T^*(\varepsilon)$ first increases, reaches a unique maximum at some $\varepsilon_0 > 0$, and then decreases. Orange domain (Case 3): if $\mathbb{T}'(\infty) > 0$, the total biomass $T^*(\varepsilon)$ is strictly increasing for all $\varepsilon > 0$. The dashed lines indicate the boundaries $\frac{dT^*}{d\varepsilon}(0) = 0$ and $\mathbb{T}'(\infty) = 0$.

Hence the sign of the slope at $\varepsilon = 0$ reflects both the asymmetry of the dispersal fluxes (via $\gamma_{12}K_2 - \gamma_{21}K_1$) and the relative growth potentials of the two patches (via $r_2(K_2 - M) - r_1$).

From (5.2), after substituting $u_1 = \dfrac{\gamma_{12}}{\gamma_{12}+\gamma_{21}}$ and $u_2 = \dfrac{\gamma_{21}}{\gamma_{12}+\gamma_{21}}$, we obtain

$$T^*(\infty) = K_1 + K_2 + \frac{N + \sqrt{\Delta}}{2r_2 u_2^3 K_1}, \tag{6.13}$$

where

$$N = \frac{-r_1\gamma_{12}^2 K_2(\gamma_{12}+\gamma_{21}) + r_2\gamma_{21}^2 K_1(K_2+M)(\gamma_{12}+\gamma_{21}) - 2r_2\gamma_{21}^3 K_1(K_1+K_2)}{(\gamma_{12}+\gamma_{21})^3},$$

and

$$\Delta = \frac{1}{(\gamma_{12}+\gamma_{21})^4}\left[\left(-\frac{r_1\gamma_{12}^2}{K_1} + r_2\gamma_{21}^2\left(1+\tfrac{M}{K_2}\right)\right)^2 + \frac{r_2\gamma_{21}^3(r_1\gamma_{12} - r_2\gamma_{21}M)}{K_2}\right].$$

Since the denominator in (6.13) is positive, the sign of $T^*(\infty) - (K_1 + K_2)$ is the same as that of $N + \sqrt{\Delta}$.

The expression (6.12) shows that the derivative at zero depends on the linear form

$$\gamma_{12}K_2 - \gamma_{21}K_1,$$

which measures the imbalance between dispersal fluxes weighted by the patch capacities. On the other hand, the numerator N in (6.13) contains the higher-order terms

$$-r_1\gamma_{12}^2 K_2(\gamma_{12}+\gamma_{21}) + r_2\gamma_{21}^2 K_1(K_2+M)(\gamma_{12}+\gamma_{21}) - 2r_2\gamma_{21}^3 K_1(K_1+K_2),$$

that can be viewed as a quadratic and cubic extension of the same combination.

Therefore, although both $\frac{dT^*}{d\varepsilon}(0)$ and $T^*(\infty)-(K_1+K_2)$ depend on the dispersal asymmetry $\gamma_{12}K_2-\gamma_{21}K_1$, the relation between their signs is not direct. In particular:

- If $N \geq 0$, then necessarily $T^*(\infty) > K_1+K_2$, so the total biomass in the infinite-diffusion regime exceeds the purely local carrying capacities. In this case, a positive initial slope in (6.12) is consistent with the asymptotic increase.
- If $N < 0$, then the contribution of $\sqrt{\Delta}$ may compensate for the negative part of N, and the sign of $T^*(\infty)-(K_1+K_2)$ depends on the delicate balance between dispersal rates and growth parameters. Consequently, the sign of $\frac{dT^*}{d\varepsilon}(0)$ does not automatically determine the asymptotic sign.

Corollary 6.8. *Assume $K_2 > M$. If*

$$-r_1\gamma_{12}^2K_2(\gamma_{12}+\gamma_{21})+r_2\gamma_{21}^2K_1(K_2+M)(\gamma_{12}+\gamma_{21})-2r_2\gamma_{21}^3K_1(K_1+K_2) \geq 0, \tag{6.14}$$

then the equilibrium biomass under infinite diffusion satisfies

$$T^*(\infty) > K_1+K_2.$$

Proof. From (6.13), we have

$$T^*(\infty)-(K_1+K_2) = \frac{N+\sqrt{\Delta}}{2r_2u_2^3K_1}.$$

Since $2r_2u_2^3K_1 > 0$, the sign is determined by $N+\sqrt{\Delta}$. If (6.14) holds, then $N \geq 0$, and because $\sqrt{\Delta} \geq 0$, we obtain $N+\sqrt{\Delta} > 0$, which proves the claim. □

7 Geometric approach to the qualitative behavior of the equilibrium point $E^*(\varepsilon)$

In this section, we adopt a geometric approach to study the qualitative behavior of the equilibrium point $E^*(\varepsilon)$ of system (3.1) as the migration rate ε varies. The analysis is based on the relative positions of the curve $\mathscr{C}$, which contains all possible equilibria, and certain reference lines in the phase plane.

Depending on the parameters, the trajectory of $E^*(\varepsilon)$ along $\mathscr{C}$ reveals whether the total equilibrium population is smaller, larger, or equal to the sum of the carrying capacities K_1+K_2 for different values of ε.

We distinguish several cases according to the slope and position of the tangent at A and of the asymptotic line $\mathscr{P}_\infty$.

We first consider the straight line Δ with Cartesian equation

$$x_1+x_2 = K_1+K_2,$$

which has slope -1 and passes through the point $A=(K_1,K_2)$.

The equilibrium point $E^*(\varepsilon)$ always lies on the curve $\mathscr{C}$ (see Appendix A). For $\varepsilon = 0$, we have $E^*(0) = A$. As ε increases, $E^*(\varepsilon)$ moves along an arc of $\mathscr{C}$ and ends at the point

$$B := E^*(\infty),$$

given by equation (5.2).

1. **Case $r_1 = r_2(K_2 - M)$.** The equation of the tangent line to $\mathscr{C}$ at A is given by:

$$(x_1 - K_1)\frac{\partial \Phi}{\partial x_1}(A) + (x_2 - K_2)\frac{\partial \Phi}{\partial x_2}(A) = 0, \tag{7.1}$$

where Φ is defined in (4.2). Since

$$\frac{\partial \Phi}{\partial x_1}(A) = -r_1, \quad \frac{\partial \Phi}{\partial x_2}(A) = (M - K_2)r_2,$$

equation (7.1) reduces to:

$$r_1 x_1 + r_2(K_2 - M)x_2 = r_1 K_1 + r_2 K_2(K_2 - M). \tag{7.2}$$

If $r_1 = r_2(K_2 - M)$, the tangent line to $\mathscr{C}$ at A coincides with Δ. By concavity of $\mathscr{C}$, all points of $\mathscr{C}$ lie below Δ. Therefore, for all $\varepsilon \geq 0$, we have:

$$x_1^*(\varepsilon) + x_2^*(\varepsilon) \leq K_1 + K_2,$$

as illustrated in Figure 7.

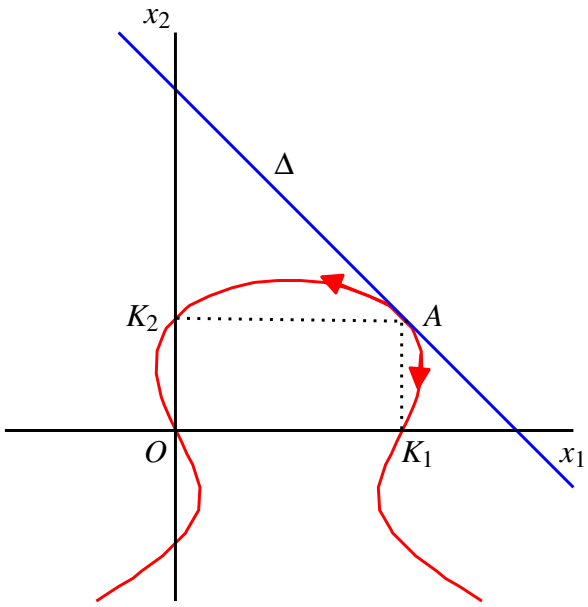

Figure 7: Illustration of item (1). The curve $\mathscr{C}$ (red) and the line Δ (blue) are shown for certain parameter values. The total equilibrium population is always smaller than $K_1 + K_2$ for all ε, since it belongs to $\mathscr{C}$. For $\varepsilon = 0$, $E^*(0) = A$; as ε increases, $E^*(\varepsilon)$ moves along $\mathscr{C}$ in one of the two directions indicated by the arrows.

2. **Case $r_1 < r_2(K_2 - M)$.** The line Δ intersects $\mathscr{C}$ at a second point C, which lies below the line $\Sigma : x_2 = \frac{K_2}{K_1} x_1$ (see Figures 8–10).

As $\varepsilon \to \infty$, the curve $\mathscr{P}_\varepsilon$ defined in (4.3) approaches the oblique line

$$\mathscr{P}_\infty : x_2 = \frac{\gamma_{21}}{\gamma_{12}} x_1.$$

The intersections of $\mathscr{P}_\infty$ with $\mathscr{C}$ are the origin and $E^*(\infty)$.

(a) If $\mathscr{P}_\infty$ lies below Σ, i.e. $\gamma_{21}/\gamma_{12} < K_2/K_1$, two situations arise:

(i) If B lies above Δ (i.e. $X_T^*(\infty) \geq K_1 + K_2$), then $E^*(\varepsilon)$ starts at A when $\varepsilon = 0$ and moves along $\mathscr{C}$ to B as $\varepsilon \to \infty$. Consequently,

$$x_1^*(\varepsilon) + x_2^*(\varepsilon) \geq K_1 + K_2, \quad \forall \varepsilon \geq 0,$$

as shown in Figure 8.

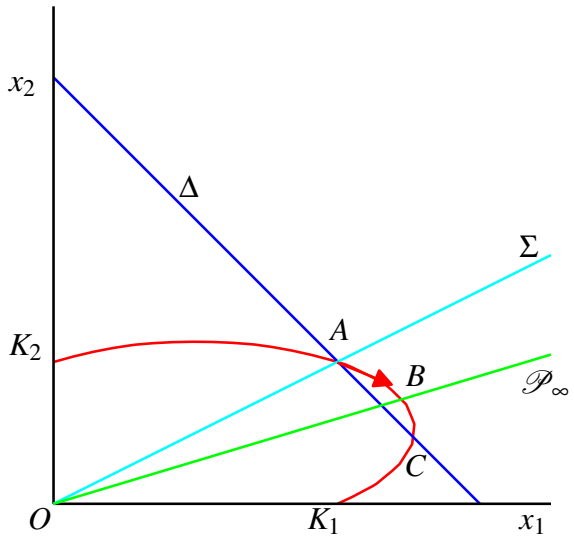

Figure 8: Illustration of item (2.a.i). The curve $\mathscr{C}$ (red), the lines Δ (blue), Σ (cyan) and $\mathscr{P}_\infty$ (green) are shown. The total equilibrium is always greater than $K_1 + K_2$ for all ε since B lies above Δ.

(ii) If B lies below Δ (i.e. $T^*(\infty) < K_1 + K_2$), then $E^*(\varepsilon)$ starts at A, passes through C at some $\varepsilon_0 > 0$, and ends at B. Thus:

$$\begin{cases} x_1^*(\varepsilon) + x_2^*(\varepsilon) > K_1 + K_2, & \varepsilon < \varepsilon_0, \\ x_1^*(\varepsilon) + x_2^*(\varepsilon) < K_1 + K_2, & \varepsilon \geq \varepsilon_0, \end{cases}$$

as illustrated in Figure 9.

(b) If $\mathscr{P}_\infty$ lies above Σ, i.e. $\gamma_{21}/\gamma_{12} > K_2/K_1$, then:

$$x_1^*(\varepsilon) + x_2^*(\varepsilon) < K_1 + K_2, \quad \forall \varepsilon,$$

as in Figure 10.

(c) If $\mathscr{P}_\infty$ coincides with Σ (i.e. $A \equiv B$), then $E^*(\varepsilon) = (K_1, K_2)$ for all $\varepsilon \geq 0$ and the total equilibrium population is constant.

8 Numerical Simulations

In this subsection, we illustrate Theorems 6.5 and 6.7 by computing the total equilibrium population $T^*(\varepsilon)$ for various parameter sets corresponding to the three monotonicity patterns.

The steady state $(x_1^*(\varepsilon), x_2^*(\varepsilon))$ is obtained by solving the equilibrium system (6.3) using a Newton–Raphson method for each $\varepsilon > 0$. Table 1 lists the baseline parameter values for the three examples.

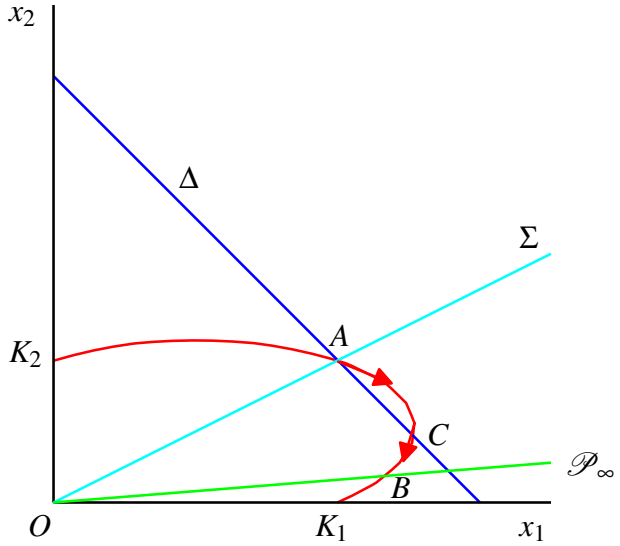

Figure 9: Illustration of item (2.a.ii). The equilibrium point $E^*(\varepsilon)$ passes through C before ending at B below Δ.

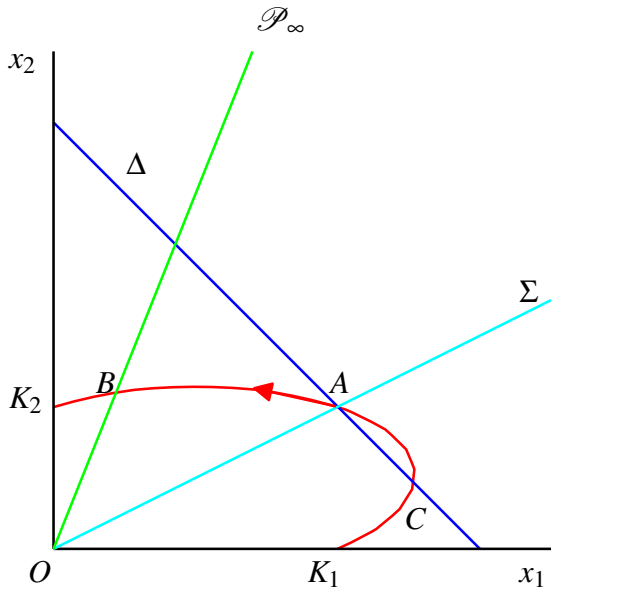

Figure 10: Illustration of item (2.b). The total equilibrium population remains smaller than $K_1 + K_2$ for all ε.

Case	r_1	r_2	K_1	K_2	M	γ_{12}	γ_{21}	Monotonicity
1	1.5	1.0	5.0	3.0	-1	0.4	0.6	Decreasing
2	1.5	0.9	5.0	3.0	-1	0.4	0.6	Unimodal
3	1.5	2.0	5.0	3.0	-1	0.4	0.6	Increasing

Table 1: Parameter values used in the simulations.

Figure 11 displays $T^*(\varepsilon)$ for $\varepsilon \in [0,5]$ in the three scenarios. In Case 1, T^* decreases monotonically, confirming Theorem 6.7(1). In Case 2, T^* is unimodal, reaching a maximum at $\varepsilon = \varepsilon_0$ as predicted by Theorem 6.7(2). In Case 3, T^* increases monotonically, illustrating Theorem 6.7(3).

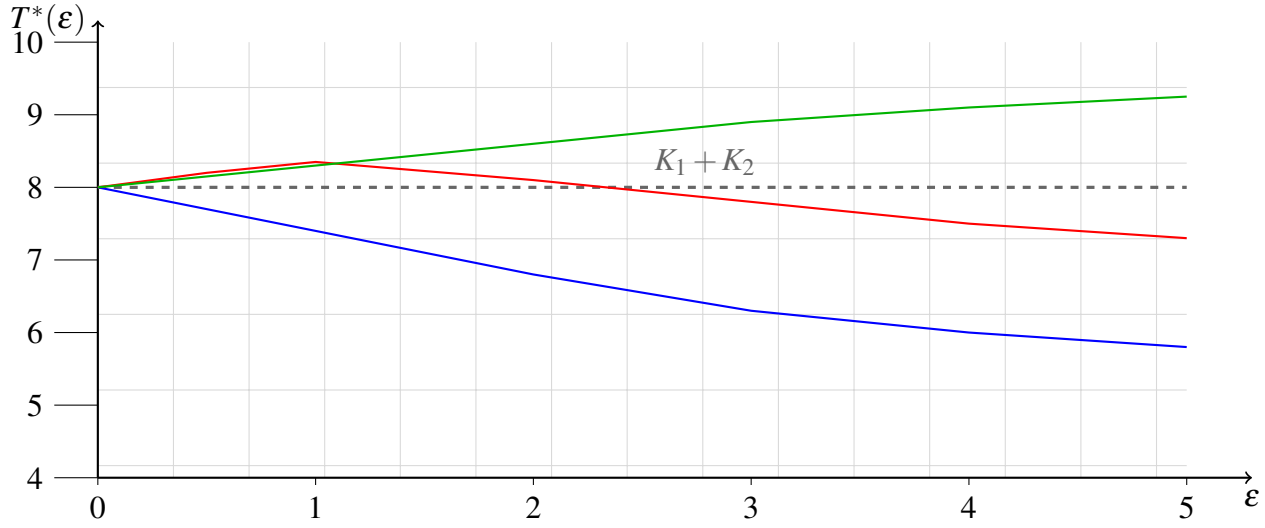

Figure 11: Numerical variation of $T^*(\varepsilon)$ for the three monotonicity cases in Table 1, with y-axis starting at 4. The dashed line indicates the baseline $T^*(0) = K_1 + K_2$.

These simulations clearly confirm the theoretical trichotomy:

- Case 1: Any dispersal reduces total biomass.
- Case 2: Moderate dispersal increases biomass up to ε_0, after which biomass declines.
- Case 3: Dispersal consistently increases total biomass.

9 Conclusion and discussion

In this work, we have investigated the influence of a weak Allee effect on the total biomass of a single-species population distributed over a patchy environment. Using a reaction–diffusion framework with patch heterogeneity, we established analytical results describing the qualitative behavior of steady states and quantified the changes in total biomass as a function of the dispersal rate. Our study shows that, under a weak Allee effect, the total biomass decreases monotonically with increasing dispersal, and no positive dispersal rate can yield the same biomass as in the absence of dispersal. These results extend previous findings obtained in purely logistic settings, highlighting that the presence of a weak Allee effect does not reverse the biomass–dispersal relationship.

From an ecological perspective, our findings emphasize that promoting movement between patches may not enhance, and may even reduce, the overall population size when a weak Allee effect is present. This has important implications for conservation strategies and habitat management, particularly in fragmented landscapes where both dispersal and Allee effects play significant roles.

Future work could address the extension of these results to multi-species interactions, more general nonlinear dispersal mechanisms, and stochastic perturbations, in order to assess the robustness of the observed biomass patterns.

Discussion on the strong Allee effect. When the weak Allee effect is replaced by a *strong* Allee effect, the mathematical analysis becomes significantly more challenging. In contrast to the weak case, where the per capita growth rate remains positive at low densities, the strong Allee effect introduces a critical threshold below which the population declines to extinction. This creates multiple equilibria in each patch (extinction, unstable threshold, and carrying capacity) and leads to the possibility of bistability. From an analytical standpoint, the existence and uniqueness of positive steady states can no longer be guaranteed by straightforward monotonicity arguments, and the total biomass may exhibit discontinuous changes as dispersal varies. Moreover, dispersal can have non-intuitive effects: it may either rescue populations from extinction or, conversely, drive them below the critical threshold in some patches. These phenomena require the use of bifurcation theory, stability switching analysis, and careful treatment of threshold dynamics, making the derivation of general biomass–dispersal relationships far more intricate than in the weak Allee effect scenario.

References

[1] R. ARDITI, C. LOBRY AND T. SARI, *Is dispersal always beneficial to carrying capacity? New insights from the multi-patch logistic equation*. Theoretical Population Biology, **106**, 45–59 (2015). DOI: 10.1016/j.tpb.2015.10.001. 2

[2] R. ARDITI, C. LOBRY AND T. SARI, *Asymmetric dispersal in the multi-patch logistic equation*. Theoretical Population Biology, **120**, 11–15 (2018). DOI: 10.1016/j.tpb.2017.12.006. 2, 12

[3] L. CHEN, T. LIU AND F. CHEN, *Stability and bifurcation in a two-patch model with additive Allee effect*. AIMS Mathematics, **7**(1), 536–551 (2021). DOI: 10.3934/math.2022034. 3

[4] B. ELBETCH, T. BENZEKRI, D. MASSART AND T. SARI, *The multi-patch logistic equation*. Discrete and Continuous Dynamical Systems - Series B, **26**(12), 6405–6424 (2020). 3

[5] B. ELBETCH, T. BENZEKRI, D. MASSART AND T. SARI, *The multi-patch logistic equation with asymmetric migration*. Revista Integración, Temas de Matemáticas, **40**(1), 25–57 (2022). 3

[6] B. ELBETCH, *Effect of dispersal in two-patch environment with Richards growth on population dynamics*. Journal of Innovative Applied Mathematics and Computer Science, **2**(3), 41–68 (2022). 3, 12

[7] B. ELBETCH AND A. MOUSSAOUI, *Nonlinear diffusion in the multi-patch logistic model*. Journal of Mathematical Biology, **87**(1) (2023). 3

[8] B. ELBETCH, *Effect of dispersal in single-species discrete diffusion systems with source-sink patches*. Mathematica Applicanda, **51**(1), 51–97 (2023). 3

[9] B. ELBETCH, *On the effect of density-dependent dispersal on the global dynamics of population*. Annals of Mathematical Sciences and Applications, **9**(2), 341–364 (2024). 3

[10] B. ELBETCH, *Effects of rapid population growth on total biomass in multi-patch environment*. Differential Equations and Applications, **15**(4), 323–359 (2023). 3

[11] B. ELBETCH, *Generalized logistic equation on networks*. Comptes Rendus Mathématique, **361**, 911–934 (2023). 3, 7

[12] B. ELBETCH, *Influence of dispersal asymmetry on total biomass in two-patch environment with generalized growth rate*. Journal of Optimization, Differential Equations and their Applications, **32**(2), 16–40 (2024). 3

[13] B. ELBETCH, *Generalized coupled source-sink models*. `https://hal.science/hal-04167884` (2023). 3

[14] H. I. FREEDMAN AND P. WALTMAN, *Mathematical Models of Population Interactions with Dispersal I: Stability of two habitats with and without a predator*. SIAM Journal on Applied Mathematics, **32**, 631–648 (1977). DOI: 10.1137/0132052. 2

[15] D. GAO AND Y. LOU, *Total biomass of a single population in two-patch environments*. Theoretical Population Biology (2022). `https://doi.org/10.1016/j.tpb.2022.05.003`. 3, 11, 14, 16

[16] D. GAO AND Y. LOU, *Impact of State-Dependent Dispersal on Disease Prevalence*. Journal of Nonlinear Science, **31**:73 (2021). `https://doi.org/10.1007/s00332-021-09731-3`. 14, 16

[17] D. GAO, *How does dispersal affect the infection size?*. SIAM Journal on Applied Mathematics, **80**(5), 2144–2169 (2020). 14

[18] C. GRUMBACH, F. N. REURIK AND J. SEGURA, *The effect of dispersal on asymptotic total population size in discrete and continuous-time two-patch models*. Journal of Mathematical Biology, **87**:60 (2023). `https://doi.org/10.1007/s00285-023-01984-8`. 3

[19] I. A. HANSKI AND M. E. GILPIN, *Metapopulation Biology: Ecology, Genetics, and Evolution*. Academic Press, 1997. 2

[20] R. D. HOLT, *Population dynamics in two patch environments: some anomalous consequences of an optimal habitat distribution*. Theoretical Population Biology, **28**, 181–201 (1985). DOI: 10.1016/0040-5809(85)90027-9. 2

[21] Y. KANG AND N. LANCHIER, *Expansion or extinction: Deterministic and stochastic two-patch models with Allee effects*. Journal of Mathematical Biology, **62**, 925–973 (2011). DOI: 10.1007/s00285-010-0359-3. 3

[22] S. A. LEVIN, *Dispersion and population interactions*. American Naturalist, **108**, 207–228 (1974). DOI: 10.1086/282900. 2

[23] S. A. LEVIN, *Spatial patterning and the structure of ecological communities, in Some Mathematical Questions in Biology VII*. Vol. **8**, Amer. Math. Soc., Providence, RI., 1976. 2

[24] S. A. LEVIN, T. M. POWELL AND J. H. STEELE, *Patch Dynamics*. Lecture Notes in Biomathematics, Vol. **96**, Springer-Verlag, 1993. 2

[25] Y. Y. LV, L. J. CHEN AND F. D. CHEN, *Stability and bifurcation in a single species logistic model with additive Allee effect and feedback control*. Advances in Difference Equations, **8**, 2686–2697 (2020). DOI: 10.1186/s13662-020-02586-0. 3

[26] Y. Y. LV, L. J. CHEN, F. D. CHEN AND Z. LI, *Stability and bifurcation in an SI epidemic model with additive Allee effect and time delay*. International Journal of Bifurcation and Chaos, **31**, 2150060 (2021). DOI: 10.1142/S0218127421500607. 3

[27] D. PAL AND G. P. SAMANTA, *Effects of dispersal speed and strong Allee effect on stability of a two-patch predator-prey model*. International Journal of Dynamics and Control, **6**, 1484–1495 (2018). DOI: 10.1007/s40435-018-0407-1. 3

[28] S. SAHA AND G. P. SAMANTA, *Influence of dispersal and strong Allee effect on a two-patch predator-prey model*. International Journal of Dynamics and Control, **7**, 1321–1349 (2019). DOI: 10.1007/s40435-018-0490-3. 3

[29] A. N. TIKHONOV, *Systems of differential equations containing small parameters in the derivatives*. Matematicheskii Sbornik, **31**, 575–586 (1952). `refhub.elsevier.com/S0040-5809(15)00102-1/sbref18`. 10

[30] W. WANG, *Population dispersal and Allee effect*. Ricerche di Matematica (2016). DOI: 10.1007/s11587-016-0273-0. 3

[31] W. R. WASOW, *Asymptotic Expansions for Ordinary Differential Equations*. Robert E. Krieger Publishing Company, Huntington, NY, 1976. 10

[32] H. WU, Y. WANG, Y. LI AND D. DEANGELIS, *Dispersal asymmetry in a two-patch system with source-sink populations*. Theoretical Population Biology, **131**, 54–65 (2020). DOI: 10.1016/j.tpb.2019.11.004. 3